

Full Length Research Paper

# Finite-element modeling and experimental study of nitrogen concentration profile in 16MnCr5 gas nitrided steel

Naim Sylja<sup>1,2</sup> and Fisnik Aliaj<sup>2\*</sup>

<sup>1</sup>University of Kadri Zeka, Zija Shemsiu Str.nn, 60000 Gjilan, Kosovo Europe.

<sup>2</sup>Department of Physics, Faculty of Mathematics and Natural Sciences (FMNS), University of Prishtina, Mother Theresa Str. 5, 10000 Prishtina, Kosovo Europe.

Received 15 September, 2015; Accepted 6 October, 2015

In this paper, a numerical and experimental study of the nitrogen concentration profile in the precipitation layer of gaseous nitrided 16MnCr5 alloy steel was performed. The gaseous nitriding was performed in ammonia atmosphere at 510, 550 and 590°C, and for each temperature four different nitriding times were chosen. Nitrogen concentration profile of the nitrided specimens was experimentally investigated with electron probe microanalysis and modeled with finite element method through ANSYS finite-element software package. The model was coded in ANSYS Parametric Design Language, and the validity of the model was demonstrated by comparison with experimental data. The accuracy of the proposed model makes it a valuable tool in complementing the experimental investigations on gaseous nitriding of 16MnCr5 and similar alloy steels.

**Key words:** Finite element method, nitrogen profile, 16MnCr5, ANSYS, electron probe microanalysis (EPMA).

## INTRODUCTION

Nitriding is an industrial thermochemical surface treatment process, usually carried out at temperatures ranging from 500 to 590°C, by which the surface of various steel materials is enriched with nitrogen that is introduced through a nitrogen donating species. This process leads to improvements in the surface properties of steels such as resistance to wear, fatigue, and corrosion. Although nitriding may be performed in gas phase (Kerr et al., 1991), liquid phase (ASM Committee on Liquid Nitriding, 1991), and plasma (O'Brien and Goodman, 1991), it is only the gaseous nitriding method that allows a precise process control of nitrogen uptake

via the chemical potential of nitrogen in the gas phase (Selg, 2012).

Gaseous nitriding is most commonly performed in ammonia (NH<sub>3</sub>) with an addition of a second gas, for example H<sub>2</sub>, N<sub>2</sub>, NH<sub>3</sub>diss, air (Małdziński and Tacikowski, 2006; Selg, 2012; Somers and Mittemeijer, 1995; Sylja et al., 2008). During gaseous nitriding the ammonia gas under the influence of the process temperature dissociates at the surface of steel and subsequently followed by atomic nitrogen diffusion into the ferrite matrix. The diffusion of atomic nitrogen leads to the formation of a nitrided zone underneath the surface of

\*Corresponding author. E-mail: fisnik.aliaj@uni-pr.edu

Author(s) agree that this article remain permanently open access under the terms of the [Creative Commons Attribution License 4.0 International License](https://creativecommons.org/licenses/by/4.0/)

**Table 1.** Chemical composition of 16MnCr5 steel (in wt.%) measured with spark emission spectrometer JY-132F.

C	Si	Mn	Cr	Mo	Al	V	P	S	Fe
0.180	0.310	1.060	0.710	0.009	0.088	0.001	0.028	0.026	balance

**Table 2.** Sample labels and gas nitriding parameters.

510°C		550°C		590°C	
Sample	Time (h)	Sample	Time (h)	Sample	Time (h)
16_1	16	16_9	9	16_17	4
16_3	36	16_11	16	16_19	9
16_5	64	16_13	36	16_21	16
16_7	100	16_15	64	16_23	36

steel and depending on the process parameters it may be subdivided into two layers: A compound layer at the surface consisting mainly of iron nitrides ( $\epsilon-Fe_{2-3}N$  and  $\gamma'-Fe_4N$ ) and a precipitation layer underneath the compound layer composed of interstitially dissolved nitrogen in combination with nitrides of alloying elements (Emami et al., 2010; Günther et al., 2004; Hosmani et al., 2008; Jung, 2011; Schacherl and Mittemeijer, 2004; Selg, 2012; Somers et al., 1989; Syla et al., 2010). The improvement in the fatigue resistance and hardness is attributed to the interstitial dissolved nitrogen in the ferrite matrix and alloying element nitride precipitates, whereas the resistance against wear and anti-corrosion properties has been ascribed to the compound layer (Emami et al., 2010; Hoffmann and Mayr, 1992; Jung, 2011; Selg, 2012).

A significant experimental effort has been made in the past decades with the aim to elucidate the influence that nitriding process parameters have on the growth of nitriding layers. Nevertheless, with a view to practice and recognizing that experimental investigations require a great amount of time and are very expensive, the development of appropriate numerical models to describe the effects that nitriding process parameters have on the nitriding layers is necessary. In particular, the finite element method has become a very powerful tool for modeling a wide range of engineering applications. A comprehensive finite element model should be time and cost effective, reduce considerably the number of experimental investigations, and in case of nitriding for example should be easily adjusted to include or fit various geometries, steels and a wide range of process parameters. Successful efforts have been made in the recent years on the modeling of the nitriding process by using various numerical approaches. However, most of the numerical studies published in literature were focused only in describing the kinetics of nitride layer growth of pure iron (Cázares et al., 2014; Hosseini et al., 2010;

Mittemeijer and Somers, 1997; Somers and Mittemeijer, 1995). Modeling the nitride layer growth in alloy steels becomes much more complicated since the model now has to describe the growth of the nitrided layers under simultaneous development of alloy element nitrides.

In the present work, finite element method (FEM) was used to model the nitrogen concentration profile in the precipitation layer (diffusion zone) of gaseous nitrided 16MnCr5 alloy steel. The model was coded in APDL (ANSYS Parametric Design Language) and the validity of the model was demonstrated by comparison with experimental data. The model can be customized very easily to include other alloy steels similar to 16MnCr5.

## EXPERIMENTAL STUDY

Disk shaped 16MnCr5 alloy steel specimens were used to experimentally investigate the nitrogen concentration profile after gaseous nitriding at selected temperatures and times. Table 1 shows the chemical composition of 16MnCr5 steel measured with spark emission spectrometer model JY-132F. Prior to gaseous nitriding, the disk shaped 16MnCr5 alloy steel specimens with dimensions  $\phi 35 \times 10$  mm were first normalized in a  $N_2$  atmosphere for 2 h at 860°C, followed by cooling in air. The specimens were then grinded on successive grades of SiC paper, starting with 320-grit and proceeding to 400-, and 600-grit papers, using water to keep the specimens cool. After the grinding procedure, the specimens were ultrasonically cleaned in acetone for 5 min, dried in hot air, and then transferred to the actual nitriding environment. The gaseous nitriding was performed in air-doped ammonia atmosphere at temperatures of 510, 550 and 590°C, and for each temperature four different nitriding times were chosen (Table 2). After gaseous nitriding, the specimens were cut in cross-section, mounted in resin, and subsequently grinded and polished with a final polishing step of 1  $\mu$ m. In order to avoid damaging and rounding off at the edges upon cross-sectional preparation, the specimens were protected by Ni-plating prior to mounting in resin. For metallographic examinations with Optical Microscopy (OM) each cross-sectioned nitrided specimen was etched in a 2% Nital solution (2 vol.%  $HNO_3$  in ethanol).

Nitrogen concentration-depth profiles of nitrided specimens were

determined with a Joel JXA-8900 RL Electron Probe Microanalyzer ( $U = 20$  kV,  $I = 40$  nA) equipped with five wavelength-dispersive spectrometers. EPMA measurements were performed on polished cross-section of the nitrated specimens, perpendicular to the surface, starting at the surface and moving with  $5 \mu\text{m}$  increments towards the inside of the specimens.

## Modeling details

### Nitrogen diffusion in steel

The diffusion of nitrogen in pure  $\alpha$ -Fe can be expressed by the second Fick's law, as follows

$$\frac{\partial C_N}{\partial t} = D_N \cdot \frac{\partial^2 C_N}{\partial z^2} \quad (1)$$

where  $C_N$  is the concentration of nitrogen dissolved in the ferrite matrix at depth  $z$ , given temperature  $T$  and time  $t$ ;  $D_N$  is the diffusion coefficient of nitrogen in the ferrite matrix and is considered as concentration independent (Selg, 2012; Somers and Mittemeijer, 1995). According to the phase diagram of Fe-N, the maximum solubility of nitrogen in  $\alpha$ -Fe is only about 0.1 wt% (Wriedt et al., 1992). However, experimental results on hardness, concentration-depth profiles of nitrogen, phase analysis, excess nitrogen and residual stress (Günther et al., 2004; Hosmani et al., 2008; Langenhan and Spies, 1992; Somers et al., 1989; Spies and Bergner, 1992; Syla et al., 2008) indicate that the percent solubility of nitrogen in the gas nitrated steels is substantially higher than in  $\alpha$ -Fe, which is attributed to the presence of alloying elements with which nitrogen forms various types of nitrides. Furthermore, alloying element nitrides may cause deformation of the crystal lattice leading to the formation of additional free space where nitrogen may dissolve. The process of atomic nitrogen diffusion in alloy steels is much more complicated than in  $\alpha$ -Fe, therefore a member was added in Equation (1) that takes into account the variations in nitrogen concentration with time as a result of alloy element nitride formation, namely:

$$\frac{\partial C_N}{\partial t} = D_N \cdot \frac{\partial^2 C_N}{\partial z^2} + \frac{\partial C_b}{\partial t} \quad (2)$$

In Equation (2),  $D_N$  is the diffusion coefficient of nitrogen in steel, which takes into account the influence of the alloying elements.

According to Spies and Bergner (1992)  $D_N = \eta \cdot D_N$ , where  $D_N = 7.8 \cdot 10^{-7} \cdot \exp(-79.1 \text{ kJ/mol RT}) \text{ m}^2/\text{s}$  is the diffusion coefficient of nitrogen in the ferrite matrix, and  $\eta$  is an empirical temperature-independent coefficient that describes the decrease in nitrogen diffusivity with alloy concentration, and for 16MnCr5 alloy steel was found to be 0.39 (Syla, 2007). The change in the concentration of nitrogen, bounded with alloying elements leading to precipitation of nitrides at the nitriding temperature, in unit of time is given by  $\partial C_b / \partial t$ . An adaptation of Robson and Bhadeshia (1997) model, which is based on the classical Johnson-Mehl-Avrami theory, was utilized for the volume change computations that accompanies the precipitation of alloying element nitrides during gaseous nitriding of steel (a parameter of crucial importance for the development of the FE model). In our case important are nitrides formed with 'free' chromium in steel, and only that of type CrN, because it has been

found experimentally that this type of nitride has the dominant influence on the increase in fatigue resistance and hardness of chromium containing steels (Hosmani et al., 2008; Syla, 2007; Syla et al., 2008). Experimental investigations with TEM, on heat treated 31CrMoV9 steel, have shown that in 31CrMoV9 steel there is approximately 1/3 of overall chromium content in free condition, whilst the rest of chromium is bounded in cementite (Syla, 2007). For 16MnCr5 steel that is the content of the present study to the best knowledge of the authors there is no such information. Following, we present a way to estimate the concentration of chromium that is able to bond with nitrogen to form CrN nitrides, and thus also the mass and volume fractions of such nitrides.

### Calculation of mass and volume fraction of CrN

To continue with the model based on Equation (2), the value of concentration corresponding to free chromium (able to bond with nitrogen and form nitrides of type CrN) had to be known. Therefore, it was assumed based on the results for 31CrMoV9 steel that the ratio of carbon to bounded chromium in 31CrMoV9 steel is equal to the ratio of carbon to bounded chromium in 16MnCr5 steel. The concentration of carbon in 31CrMoV9 steel is reported elsewhere (Syla, 2007) and amounts to 0.29 wt%. The concentration of carbon in 16MnCr5 steel is 0.18 wt% (Table 1). Hence, following the above assumptions and experimental results we have  $0.29 \text{ wt\%} : (2/3) = 0.18 \text{ wt\%} : k$ , from where we found that the fraction of the overall chromium content in 16MnCr5 ( $C_{Cr} = 0.71 \text{ wt\%}$ ) bounded in cementite is  $k = 0.41$ . So, the concentration of bounded chromium is  $0.41 \times C_{Cr}$ , whereas the concentration of free chromium is:

$$C_{Cr}^* = C_{Cr} - 0.41 \times C_{Cr} = 0.59 \times C_{Cr} = 0.59 \times 0.71 \text{ wt\%} = 0.42 \text{ wt\%} \quad (3)$$

It is easy to show that the mass fractions of chromium and nitrogen in CrN are 0.7878 and 0.2122, respectively. The mass of an individual CrN is therefore equal to 1.269 ( $1 \div 0.7878$ ) times the mass of chromium, which means that the mass fraction of all CrN precipitated during gaseous nitriding of 16MnCr5 steel will be:

$$[M_{CrN}] = C_{Cr}^* \times 1.269 \quad (4)$$

In general, during gaseous nitriding of 16MnCr5 steel, we will have two phases - the CrN and the  $\alpha$ -Fe parent phase, respectively. The mass fraction of CrN phase is therefore:

$$[M_{CrN}] = \frac{M_{CrN}}{M_{CrN} + M_{\alpha-Fe}}$$

or

$$[M_{CrN}] = \frac{1}{1 + \frac{M_{\alpha-Fe}}{M_{CrN}}} = \frac{1}{1 + \frac{V_{\alpha-Fe} \cdot \rho_{\alpha-Fe}}{V_{CrN} \cdot \rho_{CrN}}} \quad (5)$$

where  $V_{CrN}$ ,  $\rho_{CrN}$ , and  $V_{\alpha-Fe}$ ,  $\rho_{\alpha-Fe}$  are the volume and density of the CrN and  $\alpha$ -Fe, respectively. Similarly, for the volume fraction of the CrN phase we have:

$$[V_{CrN}] = \frac{V_{CrN}}{V_{CrN} + V_{\alpha-Fe}} = \frac{1}{1 + \frac{V_{\alpha-Fe}}{V_{CrN}}} \quad (6)$$

From Equation (5) we find that:

$$\frac{V_{\alpha-Fe}}{V_{CrN}} = \left( \frac{1}{[M_{CrN}]} - 1 \right) \cdot \frac{\rho_{CrN}}{\rho_{\alpha-Fe}} \quad (7)$$

After we substitute Equation (7) in Equation (6), and include the values of densities for CrN and  $\alpha$ -Fe phases ( $\rho_{CrN} = 5.90 \text{ g} \cdot \text{cm}^{-3}$  and  $\rho_{\alpha-Fe} = 7.85 \text{ g} \cdot \text{cm}^{-3}$ ), finally for the volume fraction of CrN phase we obtain:

$$[V_{CrN}] = \frac{1}{1 + \left( \frac{1}{[M_{CrN}]} - 1 \right) \times 0.752} \quad (8)$$

Having calculated the diffusion coefficient of nitrogen in steel and the concentration corresponding to free chromium, we can continue solving Equation (2) with FEM.

#### FEM solution in temperature field

The solution of Equation (2) will be sought with finite element method in the temperature field. This is possible because of the equivalence between mass and heat transport phenomena (Figure 1). The equivalent form of Equation (2) in temperature field is:

$$\frac{\partial T(z,t)}{\partial t} = \lambda \frac{\partial^2 T(z,t)}{\partial z^2} + \frac{\partial T_h(z,t)}{\partial t} \quad (9)$$

A description of the concepts and general principles involved in the solution of Equation (9) is now given. Firstly, we will suppose that there is a source from which an amount of heat (ammonia gas) is transmitted to the FE model representing the steel material, and the intensity of the transmission depends on the coefficient of thermal conductivity (diffusion coefficient) of the material. As a result of the transmission of heat, the temperature of the material (concentration of N) will increase. Then, the temperature values (concentration of N) of every node of the FE model will be analyzed after each interval,  $\Delta t$ , of integration. Secondly, it is supposed that in the volume of the material there are certain centers the function of which is that, after every interval of integration, the temperatures of the nodes that are above zero to effectively make zero, and thus to create the possibility of accepting more heat. Such centers were called 'precipice' or 'sink'. After every interval  $\Delta t$ , the nodes of the model are analyzed; if the temperatures at the nodes are not zero, these values are memorized and then effectively put to zero. This process is repeated recursively throughout the entire process, until the right conditions on the growth of CrN nitrides are satisfied. Finally, the temperature of the material is equal to the last temperature in the nodes of the model and all the 'lost' temperatures in the precipice. In reality, the intensity of precipice depends on the concentration of free Cr, the thermodynamic conditions of nucleation and growth of CrN precipitates and the contributions of Cr and N in CrN. The thermodynamic conditions for the nucleation and growth of CrN precipitates during gaseous nitriding of 16MnCr5 steel are given in our previous paper (Syla et al., 2010).

Finite element formulation of heat transfer problem represented by Equation (9) lead to the system of equations of the form:

$$[K] \cdot \{T\} = \{q\} \quad (10)$$

where,  $[K]$  is the conductance matrix,  $\{T\}$  is the temperature matrix, and  $\{q\}$  is the heat flow matrix. Solution of system of equations (10) is the temperature matrix

$$\{T\} = \begin{Bmatrix} T_1 \\ \vdots \\ T_i \\ \vdots \\ T_n \end{Bmatrix} \quad (11)$$

The elements of this matrix,  $T_i$  ( $i = 1, 2, \dots, n$ ), represent the temperatures in the nodes of the model, and are equal to the last temperature in the node and all the lost temperatures in the node  $i$ , and can explicitly be written as:

$$T_i = T_i + \sum T_h \quad (12)$$

ANSYS finite element program v10.0 was used as an environment for modeling the nitrogen depth concentration profile of the gas nitrided 16MnCr5 alloy steel. The computer model was coded in APDL (ANSYS Parametric Design Language) and was executed in the normal ANSYS environment. Solid70 element was used to model the thermal equivalent of the gas nitrided 16MnCr5 steel. Solid70 thermal solid has thermal conduction capabilities, has 8 nodes with a single degree of freedom – temperature at each node (Figure 2). The element is applicable to a 3D steady-state or transient thermal analysis.

Experimental results have shown that for the steel considered and nitriding parameters used, the maximal depth for nitrogen diffusion was approximately 1.2 mm. Therefore, a sample with length 1.5 mm and  $0.6 \times 0.6 \text{ mm}^2$  cross-section was used to model the temperature equivalent of the nitrogen depth-concentration profile of gas nitrided 16MnCr5 alloy steel. The sample model was divided into a total of 400 rectangular prism equal shaped meshes. Finite element mesh of the steel model is shown in Figure 3. Diffusion coefficients of N and Cr in steel, and a quantitative model for nucleation and growth of CrN precipitates during gaseous nitriding of steel are properly defined and entered as data in the model. More details on these aspects and other thermodynamic considerations are given in our previous study (Syla et al., 2010).

#### Volume and mass increment of CrN. precipice intensity

During finite element modeling, the total volume of nitrides was calculated as the sum of contributions from all the nodes of the model. The volume fraction of CrN phase in node "i" is written as  $AT(i)$ . According to Robson and Bhadeshia (1997), the change in extended volume during diffusion controlled growth of spherical particles (a model adapted in this paper for growth of CrN precipitates) after  $n$  sequential small increments of time is given by:

$$\Delta V_n = C \cdot V \cdot \Delta t^{5/2} \chi_n^3 \left( I_n + \frac{3}{2} \sqrt{2} \cdot I_{n-1} + \dots + \frac{3}{2} \sqrt{n} \cdot I_1 \right) \quad (13)$$

The symbols in Equation (13) have the following meaning: C is a constant equal to  $(4\pi/3)$  and the numerical subscripts identify the sequence of time increments; V is the total volume of the system;

$\Delta t$  is the increment of time;  $I_n$  is the nucleation rate per unit

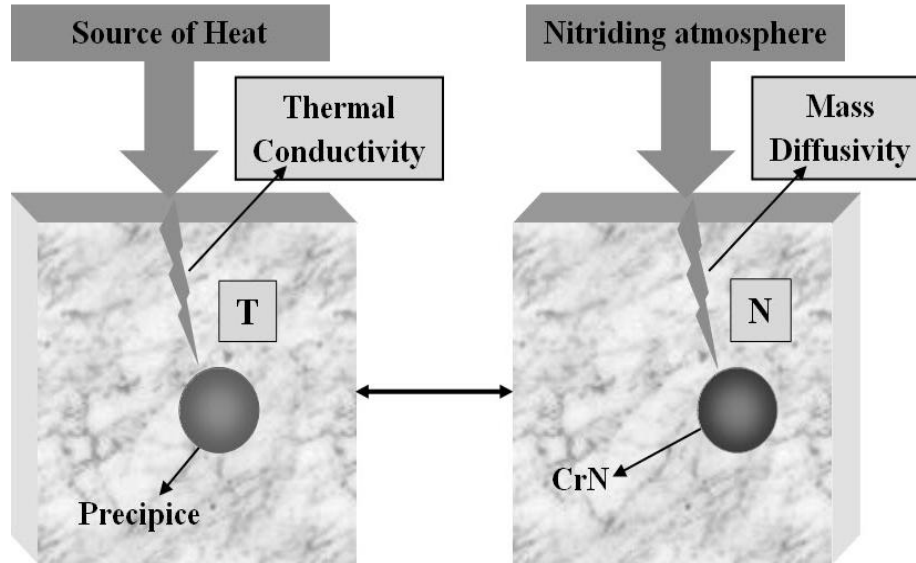


Figure 1. The analogy between the diffusion process and the imagined problem in the temperature field.

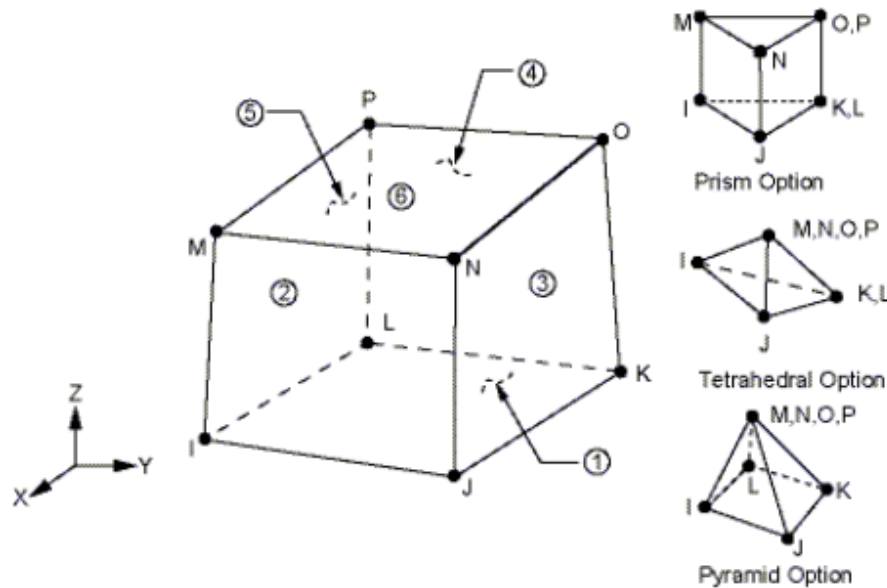


Figure 2. Solid70 element.

volume, and  $\chi_n$  is the three-dimensional parabolic rate constant.

The corresponding change in the actual volume of CrN phase in unit volume of the system is:

$$\Delta V_{CrN} = \left(1 - \sum_i AT(i)\right) \cdot \Delta V_n \quad (14)$$

Then, the new volume fraction of the CrN phase in node "n" after each increment of time is calculated recursively as:

$$AT(i) = AT(i) + \Delta V_{CrN} \quad (15)$$

This procedure is repeated for all the time intervals until the condition satisfies Equation (8). The corresponding change in the mass fraction of CrN phase as a result of the change in volume is calculated as:

$$\Delta M_{CrN} = \frac{M_{\Delta V_{CrN}}}{M_{\Delta V_{CrN}} + M_{\alpha-Fe}} = \frac{1}{1 + M_{\alpha-Fe}/M_{\Delta V_{CrN}}} \quad (16)$$

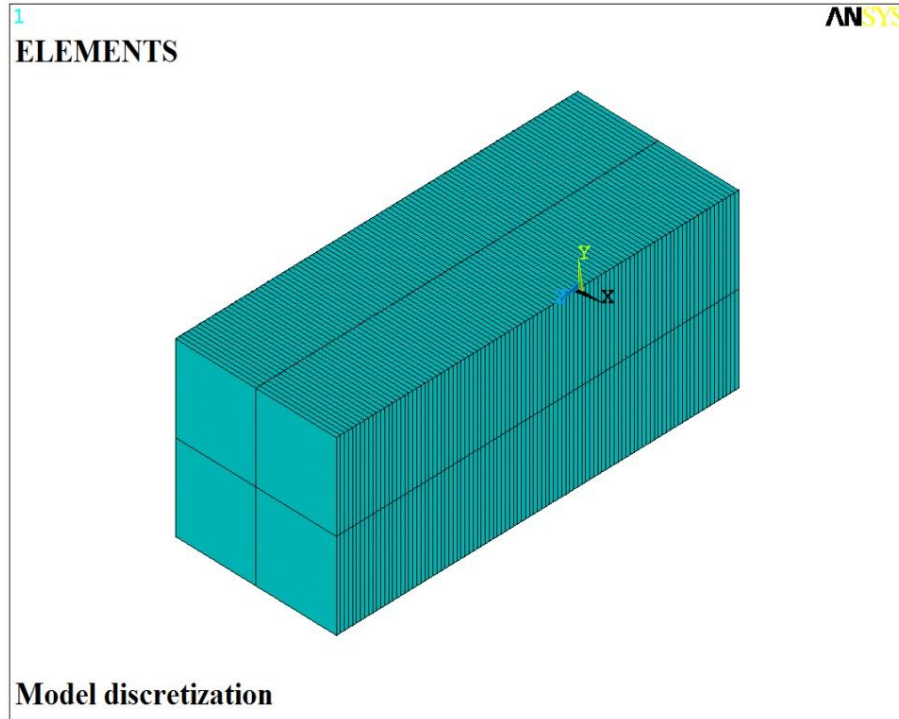


**Figure 3.** Steel sample model after meshing process. The volume of the sample is subdivided into 400 isoparametric rectangular prism finite elements.

After expressing masses as product of densities and the corresponding volumes, then finally the change in the mass fraction of CrN phase in unit volume of the system is given by:

$$\Delta M_{CrN} = \frac{1}{1 + \left( \frac{1 - \Delta V_{CrN}}{\Delta V_{CrN}} \right) \times 1.331} \quad (17)$$

The contribution of nitrogen to this change is:

$$\Delta M_N = \frac{1}{1 + \left( \frac{1 - \Delta V_{CrN}}{\Delta V_{CrN}} \right) \times 1.331} \times 0.2122 \quad (18)$$

and the rate of contribution of nitrogen to the mass increment of CrN, or equivalently the change in the concentration of nitrogen bounded to chromium in each increment of time is

$$\frac{\Delta M_N}{\Delta t} = \frac{1}{1 + \left( \frac{1 - \Delta V_{CrN}}{\Delta V_{CrN}} \right) \times 1.331} \times 0.2122 \quad (19)$$

The total nitrogen concentration is then calculated as: nitrogen bounded in chromium and nitrogen dissolved in  $\alpha$ -Fe lattice. In fact Equation (19) represents the precipitate intensity or the condition of "filling" the precipitate with heat.

## RESULTS AND DISCUSSION

The results of modeling with ANSYS are temperature equivalents of nitrogen concentrations as a function of depth. Figure 4 shows a typical finite element analysis result obtained with ANSYS for the case of the steel specimen nitrided at 510°C for 16 h (sample 16\_1). Figure 4a shows the result of the finite element analysis in a form of a diffusion contour for nitrogen, while Figure 4b depicts the nitrogen concentration-depth profile for the same specimen (in the temperature field). Nitrogen concentration-depth profiles were also obtained experimentally with EPMA. Although the phenomena of heat flow and diffusion are basically the same (are described by the same set of differential equations), there is no direct correspondence between physical parameters and variables. Thus, the results of modeling and experiment cannot be compared with each other on an absolute scale. Therefore, both of the concentration profiles (from the model and experiment) were normalized by dividing with the maximal value of concentration. Figure 5 depicts the normalized nitrogen concentration profiles of selected specimens investigated in this work. Light optical micrographs of the same specimens are shown in Figure 6, which clearly depict the nitrided zone and the un-nitrided core. From Figure 5 we can clearly see that there is a good agreement between the results of modeling and experiment, which is

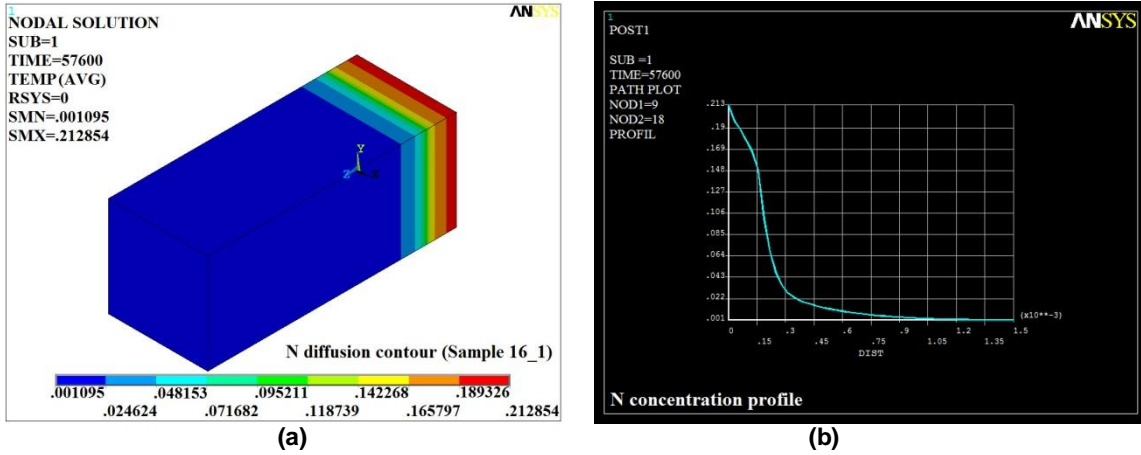


Figure 4. ANSYS results for 16MnCr5 steel specimen nitrided at 510°C for 16 h (specimen 16\_1). (a) Nitrogen diffusion contour; (b) Nitrogen concentration profile.

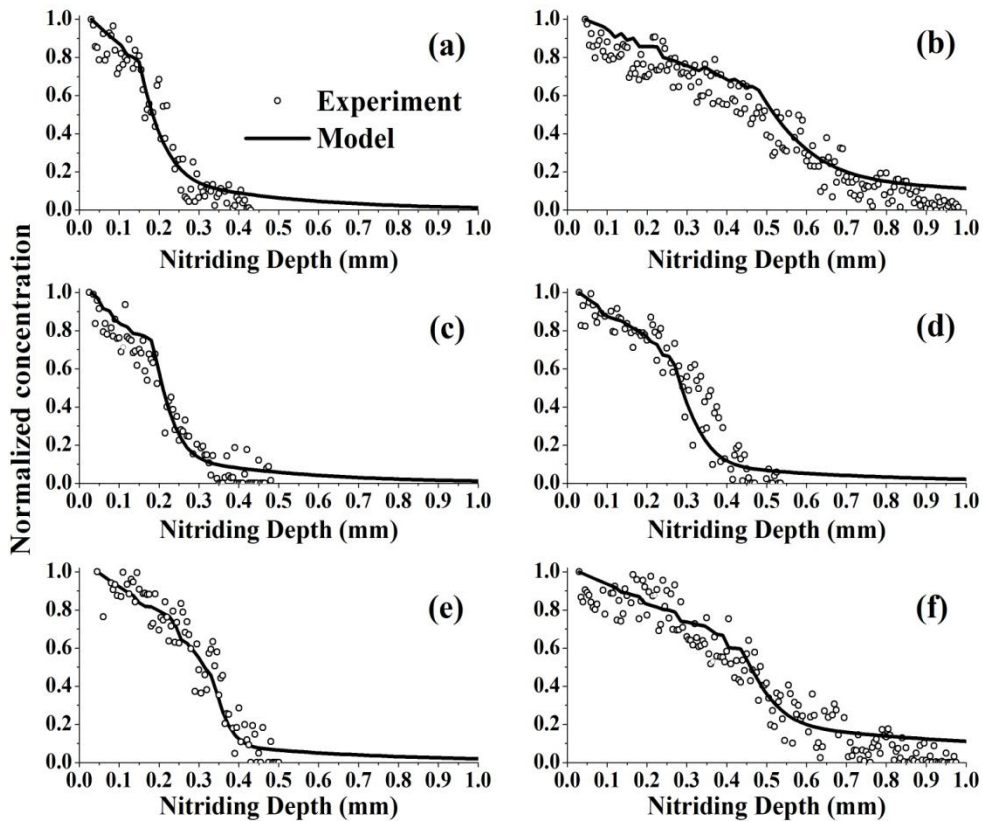
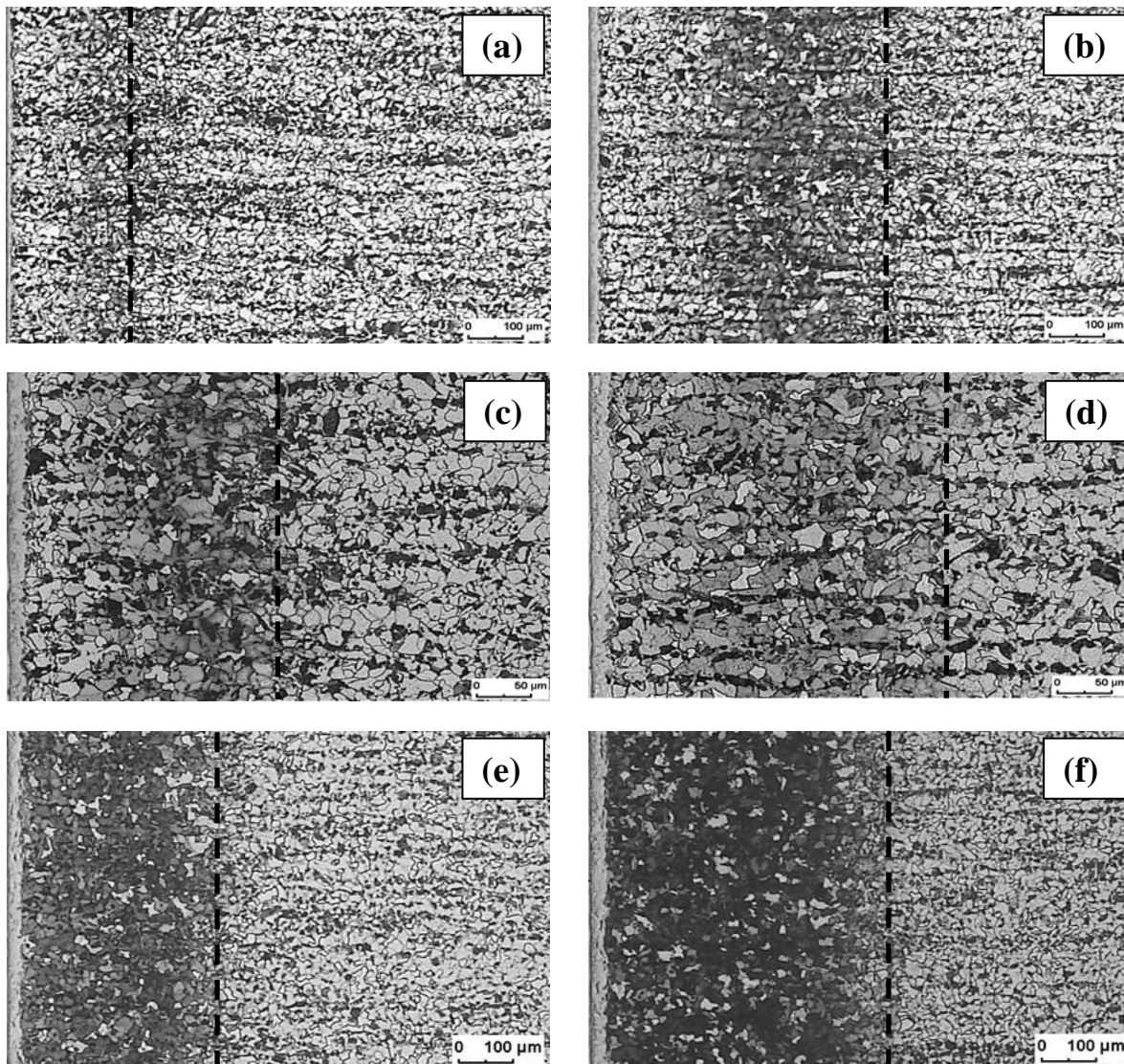


Figure 5. Normalized concentration of nitrogen as a function of nitriding depth for selected specimens investigated in this work: (a) 16\_1 (510°C, 16 h), (b) 16\_7 (510°C, 100 h), (c) 16\_9 (550 °C, 9 h), (d) 16\_11 (550°C, 16 h), (e) 16\_19 (590°C, 9 h), (f) 16\_21 (590°C, 16 h), Solid lines represent model nitrogen profiles obtained with ANSYS, while open circles represent experimental data obtained with EPMA.

an indication that our approach to the problem was correct. The differences between the results obtained experimentally and from the model may have the

following reasons.

The concentration of free Cr that is able to bond with nitrogen to form CrN precipitates was estimated based on



**Figure 6.** Light optical micrographs of the nitrided steel specimens shown in Figure 5. The nitrided zone and the un-nitrided core are clearly distinguishable. The extent of the nitrided zone has been marked with a dashed line.

the results of 31CrMoV9 steel. While this assumption proved to be correct in terms of the results obtained, differences may occur. Accordingly, additional experiments on 16MnCr5 alloy steel with the aim to elucidate the true free Cr content would greatly improve the results of the model.

CrN precipitates were assumed to grow as spherical particles according to a model developed by Robson and Bhadeshia (1997) which is based on a classical Johnson-Mehl-Avrami theory. However, during gaseous nitriding of steels containing nitride forming elements, nitriding precipitates of platelet morphology develop in the nitrided zone. These alloy element nitride platelets may have lengths up to hundred of nanometers and thicknesses of several tens of nanometers, depending on the nitride

forming alloy element concentrations and nitriding parameters (Jung, 2011; Selg, 2012). Platelet precipitate growth can be modeled with a proper modification of the expression for the extended volume during diffusion controlled growth of particles, Equation (13). The basic method is the same; the modification consists in finding the platelet aspect ratio, which may be done by means of experimental investigations or theoretical considerations.

A more sensitive analysis can be conducted by dividing the Solid70 element into a greater number of elements. This approach can be used at the risk of increasing the computational time.

Effect of pore development during nitriding of 16MnCr5 steel was not taken into account. According to Scharchel (2004), all gaseous nitride Fe-Cr alloys contain more

nitrogen than necessary for precipitation of all Cr as CrN and for realization of the equilibrium dissolution of N in the ferrite matrix. This excess nitrogen precipitates as N<sub>2</sub> gas causing pores on prolonged nitriding where the discontinuous precipitation reaction occurs and/or coarsening of the CrN precipitates becomes appreciable. All these processes cause local variations of Cr and N in the immediate surroundings of the pores, which may be another reason for the observed differences between the result of the experiment and the model.

## Conclusions

1. It was shown that the differential equation that describes the diffusion of nitrogen in 16MnCr5 alloy steel can be solved with Finite Element Method by using ANSYS in the temperature field;
2. Apart from making several approximations, such as:

- i. CrN precipitations grow as spherical particles,
- ii. Concentration of free Cr was estimated based on results for 31CrMoV9 steel,
- iii. Only nitrides of type CrN were considered, and
- iv. Effect of pores was not taken into account,

it was found that the nitrogen concentration profiles obtained by FEM were in good agreement with experimental nitrogen profiles obtained by EPMA, which is an indication that our approach to the problem was correct. The model is then applicable to various nitriding treatments and can be used as a practical tool to estimate the nitrogen concentration profile in the precipitation layer of gas nitrided 16MnCr5 steel.

3. In summary, it was observed that the results obtained from the experimental investigations with EPMA are in good agreement with the results obtained from the FE model that was written in APDL and was run in ANSYS finite element program. Furthermore, our model can be very easily customized to include other process parameters, geometries, and alloys steels similar to 16MnCr5.

4. To the best of the authors' knowledge, this work is the first to report on the modeling with ANSYS of the nitrogen concentration profile in the gas nitrided 16MnCr5 alloy steel. Our future work will focus on modeling the nitrogen concentration profile in other alloy steels and taking into account as many real processes as possible - the limit depending only on the capacity of the computers being used for modeling.

## Conflict of Interest

The authors have not declared any conflict of interest.

## REFERENCES

- ASM Committee on Liquid Nitriding (1991). ASM Handbook: Heat Treating, Vol.4. Metal Park, OH: ASM International, pp. 923-943.
- Cázares FL, Ceniceros AJ, Pena JO, Aranguren FC (2014). Modeling surface processes and kinetics of compound layer formation during plasma nitriding of pure iron. *Rev. Mex. Fis.* 60(3):257-268.
- Emami M, Ghasemi HM, Rassizadehghani J (2010). High temperature tribological behavior of 31CrMoV9 gas nitrided steel. *Surf. Eng.* 26(3):168-172.
- Günther D, Hoffmann F, Hirsch T (2004). Entstehung und Ursachen von Eigenspannungen beim Gasnitrieren chromlegierter Stähle. *Härtereitechnische Mitteilungen* 59(1):18-27. <http://dx.doi.org/>
- Hoffmann FT, Mayr P (1992). ASM Handbook: Friction, Lubrication, and Wear Technology, Metal Park, OH: ASM International, 18:1783-1796.
- Hosmani SS, Schacherl RE, Mittemeijer EJ (2008). Nitrogen absorption by Fe-1.04at.%Cr alloy: uptake of excess nitrogen. *J. Mater. Sci.* 43(8):2618-2624.
- Hosseini SR, Ashrafzadeh F, Kermanpur A (2010). Calculation and experimentation of the compound layer thickness in gas and plasma nitriding of iron. *Iran. J. Sci. Technol.* 34(B5):553-566.
- Jung KS (2011). Nitriding of iron-based ternary alloys: Fe-Cr-Ti and Fe-Cr-Al. PhD dissertation, University of Stuttgart, Germany.
- Kerr CH, Rose ThC, Filkowski JH (1991). ASM Handbook: Heat Treating, Vol.4. Metal Park, OH: ASM International, pp. 880-922.
- Langenhan B, Spies HJ (1992). Einfluß der Nitrierbedingungen auf Morphologie und Struktur von Verbindungsschichten auf Vergütungsstählen. *Härtereitechnische Mitteilungen* 47(6):337-343.
- Maldziński L, Tacikowski J (2006). Concept of an economical and ecological process of gas nitriding of steel. *Härtereitechnische Mitteilungen*, 61(6):296-302.
- Mittemeijer EJ, Somers MAJ (1997). Thermodynamics, kinetics, and process control of nitriding. *Surf. Eng.* 13(6):483-497.
- O'Brien JM, Goodman D (1991). ASM Handbook: Heat Treating, Metal Park, OH: ASM International, 4:944-954.
- Robson JD, Bhadeshia HKDH (1997). Modelling precipitation sequences in power plant steels Part1 – Kinetic Theory. *Mater. Sci. Technol.* 13(8):631-639.
- Schacherl RE, Mittemeijer EJ (2004). Nitrieren von Fe-Cr-Legierungen: Überschussstickstoff und Kinetik des Nitrierschichtwachstums. *HTM Zeitschrift für Werkstoffe Wärmebehandlung Fertigung* 59(5):312-319.
- Schacherl RE (2004). Growth Kinetics and Microstructure of Gaseous Nitrided Iron Chromium Alloys. PhD dissertation. University of Stuttgart, Germany.
- Selg H (2012). Nitriding of Fe-Mo Alloys and Maraging Steel: Structure, Morphology and Kinetics of Nitride Precipitation. PhD dissertation, University of Stuttgart, Germany.
- Somers MAJ, Lankreijer RM, Mittemeijer EJ (1989). Excess nitrogen in the ferrite matrix of nitrided binary iron-based alloys. *Philos. Mag. A*, 59(2):353-378.
- Somers MAJ, Mittemeijer EJ (1995). Layer-Growth Kinetics on Gaseous Nitriding of Pure Iron: Evaluation of Diffusion Coefficients for Nitrogen in Iron Nitrides. *Metall. Mater. Trans. A*, 26A(1):57-74.
- Spies H-J, Bergner D (1992). Innere Nitrierung von Eisenwerkstoffen. *Härtereitechnische Mitteilungen* 47(6):346-356.
- Syla N (2007). Modelimi i krijimit të veçimeve gjatë procesit të nitrimin në gazra të çelikut me përlidhje kromi. PhD dissertation (in Albanian), University of Tirana, Albania.
- Syla N, Klinaku Sh, Aliaj F (2010). Modeling of the Precipitation Layer by the Method of Finite Elements during the Process of Gaseous Nitriding of Steel 16MnCr5. *Res. J. Appl. Sci.* 5(6):444-450.
- Syla N, Schreiber G, Oettel H, Dilo T (2008). Experimental Study of the Nitriding Layer by Steel 17CrMoV10. *J. Eng. Appl. Sci.* 3(10):754-757.
- Wriedt HA, Gokcen NA, Nafziger RH (1992). ASM Handbook: Alloy Phase Diagrams,. Metal Park, OH: ASM International, 3:198.